Exp Brain Res (2010) 203:181–191
DOI 10.1007/s00221-010-2223-5

RESEARCH ARTICLE

Temporal and spatial patterns of cortical activation during assisted lower limb movement

M. Wieser · J. Haefeli · L. Bütler · L. Jäncke · R. Riener · S. Koeneke

Received: 17 April 2009 / Accepted: 8 March 2010 / Published online: 3 April 2010

Abstract Human gait is a complex process in the central nervous system that results from the integrity of various mechanisms, including different cortical and subcortical structures. In the present study, we investigated cortical activity during lower limb movement using EEG. Assisted by a dynamic tilt table, all subjects performed standardized stepping movements in an upright position. Source localization of the movement-related potential in relation to spontaneous EEG showed activity in brain regions classically associated with human gait such as the primary motor cortex, the premotor cortex, the supplementary motor cortex, the cingulate cortex, the primary somatosensory cortex and the somatosensory association cortex. Further, we observed a task-related power decrease in the alpha and beta frequency band at electrodes overlying the leg motor area. A temporal activation and deactivation of the involved brain regions as well as the chronological sequence of the movement-related potential could be mapped to specific phases of the gait-like leg movement. We showed that most cortical capacity is needed for changing the direction between the flexion and extension phase. An enhanced understanding of the human gait will provide a basis to improve applications in the field of neurorehabilitation and brain–computer interfaces.

Keywords Human leg movement · EEG · Cortical activity · Temporal and spatial patterns

M. Wieser (✉) · J. Haefeli · L. Bütler · R. Riener
Sensory-Motor Systems (SMS) Lab, Institute of Robotics and Intelligent Systems (IRIS), ETH Zurich, Tannenstrasse 1, 8092 Zurich, Switzerland
e-mail: wieser@mavt.ethz.ch

M. Wieser · R. Riener
Medical Faculty, Balgrist University Hospital, University of Zurich, Zurich, Switzerland

J. Haefeli
Institute of Human Movement Sciences and Sport, ETH Zurich, Zurich, Switzerland

L. Bütler
HUMAINE Clinic, Zihlschlacht, Switzerland

L. Jäncke · S. Koeneke
Division Neuropsychology, Institute of Psychology, University of Zurich, Zurich, Switzerland

Introduction

Experimental studies indicated that bipedal gait is controlled by spinal pattern generators and multiple motor centers in the brainstem (Armstrong 1988; Duysens and Van de Crommert 1998; Dietz 2003). Additionally, it was also shown that human gait relies on complex control mechanisms in the central nervous system and demands the contribution of different cortical and subcortical structures (Fukuyama et al. 1997; Dietz 2003; Hanakawa 2006). However, current knowledge about the neural control of gait is still limited, as the measurement of the underlying cerebral activity is challenging. Especially upright stance during walking and walking-induced head movements are limiting factors for many of the common functional neuroimaging techniques like positron emission tomography (PET), functional magnetic resonance imaging (fMRI) or electroencephalography (EEG). Past studies addressing human gait adopted alternative strategies to overcome methodological difficulties, such as limiting the research focus to the phase of gait initiation (Yazawa et al. 1997) or analyzing motor imagery of gait (Miyai et al. 2001; Malouin et al. 2003; Jahn et al. 2004; Sacco et al. 2006).

In these studies, motor planning processes were of key interest. Other studies investigated real movement execution; however, in these cases, gait was reduced to elementary foot or leg movements, such as repetitive flexion/extension (Miyai et al. 2001; Dobkin et al. 2004; Sahyoun et al. 2004; Ciccarelli et al. 2005). Using tasks that share some cerebral processes with gait is the fundamental idea of all these studies.

So far, only very few studies conducted their measurements under the condition of real voluntary human walking. Fukuyama et al. (1997) evaluated changes in brain activity as a result of walking using single photon emission tomography (SPECT). They identified the supplementary motor cortex (SMA), the primary somatosensory cortex (S1), the primary motor cortex (M1) as well as the cerebellum and parts of the basal ganglia as being involved in the higher control mechanisms of bipedal gait. Another SPECT study investigated gait-induced cortical activation on a treadmill (Hanakawa et al. 1999b) and found an expanded cortical network comprising the premotor cortex (PMC), the somatosensory association cortex (SA), the cingulate cortex (CC) and the brainstem in addition to the structures reported by Fukuyama et al. (1997). In both SPECT studies, task execution (walking) was carried out prior to image acquisition. Using near-infrared spectroscopy (NIRS), Miyai et al. (2001) studied gait on a treadmill and found gait-related activity in S1, M1 and SMA, thus corroborating earlier findings of Fukuyama et al. To our knowledge, NIRS is the only technique to date that has been applied to carry out gait performance and image acquisition simultaneously (Miyai et al. 2001; Suzuki et al. 2004, 2008; Harada et al. 2009). Unfortunately, there are well-known limitations of this technique, and in the study of Miyai et al. (2001), spatial distribution and intensity of the gait-induced metabolic changes were not statistically evaluated. Based on previous work, we therefore arrive at the conclusion that a reliable real-time image of the brain structures involved in controlling human gait has not yet been accomplished. In addition, the temporal pattern of neural activity during the gait cycle remains an open question.

The present study investigated cortical activity during lower limb movement by means of EEG, which provides a high temporal resolution, in combination with the calculation of intracerebral sources (sLORETA). With the assistance of a dynamic tilt table, all subjects performed standardized gait-like leg movements in an upright position. Moreover, the dynamic tilt table is designed for therapeutic purposes in a very early phase of neurorehabilitation. During the rehabilitation process, it seems to be important to emphasis on mobilization as early as possible (Bernhardt et al. 2007). Activation of neuronal networks associated with walking could be one of the most important features in such a rehabilitation phase. Finally, it was shown in patients with hemiparetic stroke (Miyai et al. 2002, 2003), patients with Parkinson's disease (Hanakawa et al. 1999a) and subjects with gait disturbance due to white matter changes (Iseki et al. 2010) that an enhanced premotor activation was associated with locomotor performance. This suggests that the prefrontal and premotor cortices are involved in the control of human walking. Hence, we aim to prove whether the dynamic tilt table activates brain regions classically associated with human gait and further, we hypothesize that spatial and temporal patterns of cortical activation can be assigned to explicit phases in the gait cycle.

Materials and methods

Subjects

Twenty healthy volunteers (11 women and 9 men) with a mean age of 28.6 years (SD: ± 8.3 years) and without any history of neurological, psychiatric or cardiovascular disorders took part in the study. All subjects were right-handed. The footedness was not tested separately as the right-handedness is significantly associated with right-footedness (Dittmar 2002). The local ethics committee of Canton Thurgau, Switzerland, approved the study, and each participant gave written informed consent. Tasks and testing procedures were in accordance with institutional guidelines and the study conformed to the Declaration of Helsinki. The measurements were taken at the HUMAINE Clinic, Zihlschlacht, Switzerland.

Experimental protocol

As illustrated in Fig. 1 (upper panel), the experimental session started with a resting period of 7 min. During this period, subjects were laying in a horizontal position on the *Erigo* tilt table (Hocoma AG, Switzerland), which was adjusted to $\alpha_{tilt} = 0°$. There was no motor activity of the legs during this time ($f_{step} = 0$ Hz), and subjects were asked to keep their eyes open. After this resting period and a short subsequent adaption phase, subjects performed automated gait-like stepping movements during the movement period. The movements were carried out on the *Erigo*, a system that combines a tilt table with an integrated motor-driven stepping principle (Fig. 1, lower panel). The *Erigo* was tilted to $\alpha_{tilt} = 76°$, and leg movement was adjusted to 44 steps per minute (for one leg: $f_{step} = 0.36$ Hz). After 30 min of continuous leg movement, the *Erigo* was tilted back to $\alpha_{tilt} = 0°$ and leg movement was stopped. The experimental session ended with a second resting period, which was identical to the

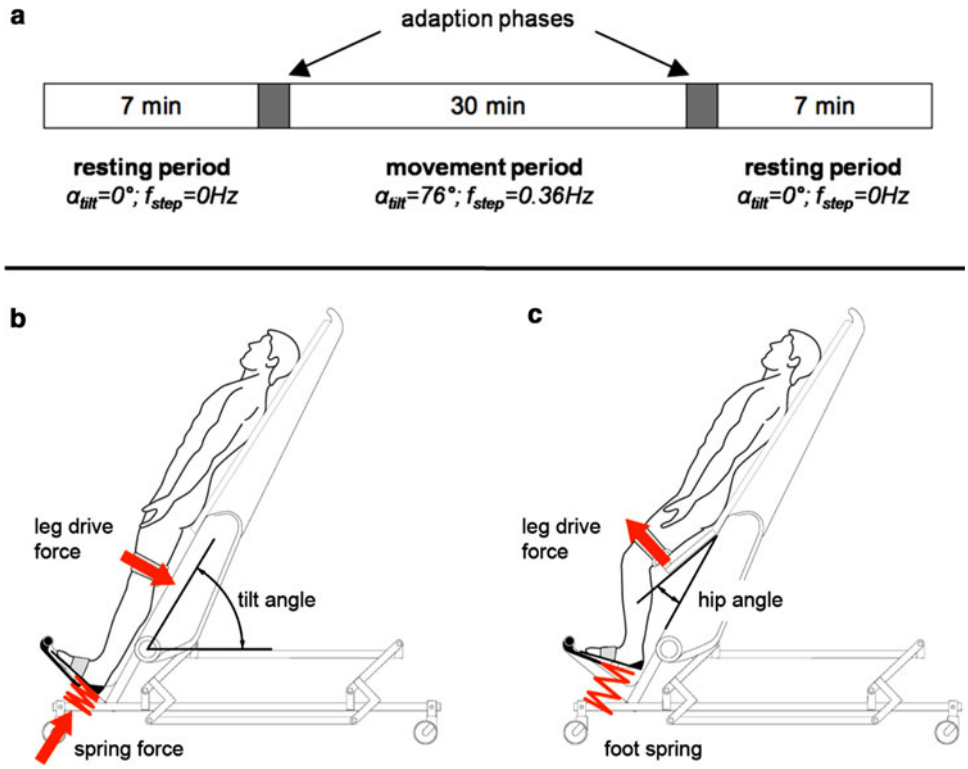

Fig. 1 Experimental protocol (**a**) with resting periods, adaption phases and movement period (*upper panel*) and the tilt table *Erigo* during extension (**b**) and flexion (**c**) (*lower panel*)

initial resting period. Subjects kept their eyes open during the entire experimental session, and EEG was recorded continuously during the whole experiment.

Erigo-assisted leg movements

The *Erigo* is driven in a sinusoidal function of time referring to the hip angle (Fig. 2). The duration of extension and flexion phase is identical and legs move conversely to each other at a constant speed. Maximal extension of one leg occurs at a hip angle of 0°. At the same time, the other leg performs a maximal flexion at the largest possible hip angle, and subsequently, both legs change the direction: from the extension to the flexion phase or from the flexion to the extension phase, respectively. After every extension phase of the left leg, a time marker is given by the Erigo in order to perform accurate averaging of the acquired data. Due to different lengths of the lower extremities, the maximal hip angle varies among subjects, whereas the Erigo is adjustable to the individual leg length of the subject. We normalized the absolute hip angle (0° → 0%; max. individual hip angle → 100%) to analyze the averaged relative leg movement of all subjects.

In order to avoid movement artifacts in the EEG recordings, the trunk and hip were tightly fixed by a belt system and the head was stabilized with a neck cushion that is shapable according to the individual needs of the subjects. The feet were attached on two separate mobile footplates and Velcro strips fastened the leg to an end-effector of the Erigo in order to perform reproducible standardized movements. Comparable to real human gait, the *Erigo* allows a highly synchronized movement of the hip, knee and ankle of the left and right leg. In contrast to real human gait, however, subjects move their legs only in horizontal but not in vertical direction.

To classify the degree of activity during the *Erigo*-assisted leg movements, electromyographic activity (EMG) was recorded in four involved leg muscles (rectus femoris, biceps femoris, tibialis anterior and gastrocnemius medialis) in eight subjects during the movement period (uninstructed condition: ASSISTED condition) and during two additional instructed movement conditions performed after the actual experimental session. In the first instructed condition, the subject was asked to relax and remain passive while the movement was performed by the *Erigo* (PASSIVE). So, 100% guidance was provided during the PASSIVE condition, and lower limbs were moved by the stepping device without any effort coming from the subject. In the second instructed condition, the stepping device provided only the rhythm and the subject was requested to participate as active as possible (ACTIVE).

EEG and EMG data acquisition

During the two resting periods and the intermediate movement period, EEG was continuously recorded from 64

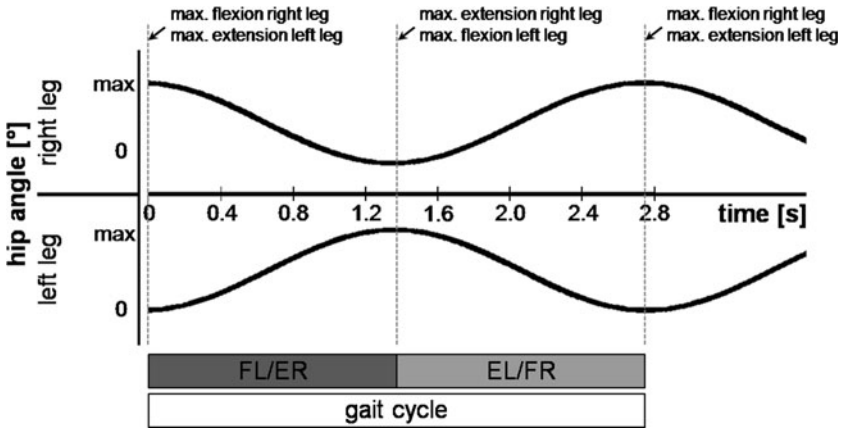

Fig. 2 The hip angle of both legs relative to the gait cycle. The gait cycle consists of two phases. In the first part, the *left leg* performs a flexion and the *right leg* an extension (FL/ER), whereas in the second part, the *left leg* performs an extension and the *right leg* a flexion (EL/FR)

scalp electrodes using a SynAmps^2 amplifier system (Compumedics Neuroscan, Germany). Silver-silver-chloride electrodes were used in combination with a SynAmps^2 Quik-Cap (Compumedics Neuroscan, Germany) and were placed in the following positions according to the international 10–20 electrode placement standard: Fp1/2, Fpz, AF3/4, F1/2/3/4/5/6/7/8, Fz, FC1/2/3/4/5/6/7/8, FCz, C1/2/3/4/5/6/7/8, Cz, CP1/2/3/4/5/6/7/8, CPz, P1/2/3/4/5/6/7/8, Pz, PO3/4/5/6/7/8, POz, O1/2, Oz, CB1/2. The reference electrode was located between Cz and CPz. The electro-oculogram (EOG) was recorded from two pairs of bipolar electrodes placed below the outer canthi of each eye in order to detect horizontal eye movements as well as above and below the center of one eye to record vertical eye movements. The software package Scan 4.2 (Compumedics Neuroscan, Germany) was used to record and store the acquired data. Electrode impedance was kept below 10 kΩ. Data were sampled at 1000 Hz, and the lower and upper cut-off frequencies were 0.5 and 70 Hz, respectively.

The EMG of the four muscles was recorded with a TeleMyo^{TM} DTS System (Noraxon, USA). This system transmits EMG data directly from the electrode to a receiver via Direct Transmission Telemetry. The software package MyoResearch XP (Noraxon, USA) was used to acquire and store the EMG data with a sampling frequency of 1500 Hz.

EEG and EMG data analysis

The recorded EEG data were further processed off-line using the BrainVision Analyzer software package (Brainproducts, Germany).

EEG data were bandpass filtered from 1.5 to 30 Hz (Butterworth), and data were re-referenced to an average reference of all electrodes. Ocular artifacts (eye blinks, horizontal eye movements) were corrected applying an independent component analysis (ICA) algorithm provided by the BrainVision software. Thereafter, EEG data were searched for epochs containing artifacts that exceed ±100 μV at any electrode. Those epochs were also excluded from subsequent analysis.

EEG data were segmented into epochs of 2.75 s identical to the length of one gait cycle. These segments were averaged relative to gait cycle and electrode position. The mean number of epochs per average was 500 (SD: ± 126). Individual waveforms were averaged to a single grand average movement-related potential. Subsequently, the gait cycle was divided into two periods of equal lengths: In the first period, the left leg performs a flexion and the right leg performs an extension (FL/ER), while in the second period of the gait cycle, the left leg performs an extension and the right leg a flexion (EL/FR). The shape of the grand average waveform at the Cz electrode as well as the topographical scalp maps was visually inspected for recurrent patterns.

The movement-related potential and the spontaneous EEG signal recorded during the two resting periods were imported into the sLORETA software (http://www.uzh.ch/keyinst/loreta.htm) in order to compute intracerebral sources of activity. sLORETA is an instantaneous, 3D, discrete, linear solution for the EEG inverse problem that allows the quantitative neuroanatomical localization of neuronal electric activity by assuming that neighboring neural sources show similar activation patterns. For the localization, a three-shell spherical head model registered to the Talairach human brain atlas (Talairach and Tournoux 1988) is used. Brodmann areas (BAs) were identified on the basis of a lookup table with a clear mapping between voxels and corresponding BAs. A review on different methods for solving the EEG inverse problem as well as the corresponding mathematical solution is given by Pascual-Marqui et al. (1999, 2002); Pascual-Marqui 2002). The cerebral sources of the movement period (30 min of continuous stepping) were compared with those of the pre- and post-resting periods (14 min in total) by means of a paired *t*-test on log-transformed data.

Further, the movement-related potentials of the two gait cycle periods (FL/ER and EL/FR) were averaged. In the resulting waveform, local minima and maxima at the Cz electrode, an electrode likely overlying the leg sensorimotor cortex, were detected. By use of the sLORETA software, source localization was performed at the detected extreme values with a time frame of ±25 ms. Thus, significantly active brain regions at the specific time intervals were analyzed.

In an alternative analysis, a fast Fourier transform (FFT) algorithm (Hanning window) was applied to the artifact-free EEG signal. The EEG signal was filtered and segmented into epochs of 2.75 s, separately for the rest and movement period. The power spectrum from 1.5 to 30 Hz was calculated for each single epoch and then averaged for each subject and task condition. The mean spectral power in the alpha (8–12 Hz) and beta frequency band (13–30 Hz) during movement and resting periods at electrodes overlying the leg motor area (pooled Cz and CPz electrodes) was analyzed, and task-related band power decrease (TRPD) and increase (TRPI) was determined (Gerloff et al. 1998; Manganotti et al. 1998; Andres et al. 1999; Hummel et al. 2002). TRPD/TRPI concentrates on changes with steady-state processes related to continuous movement execution or mental imagery (Hummel and Gerloff 2006; Neuper et al. 2006). Hence, this analysis basically served to confirm data reliability and quality.

EMG signals, obtained from eight subjects, were rectified (RMS algorithm, window: 50 ms) and segmented into epochs of 2.75 s, which is in accordance with the duration of one gait cycle. In addition, the segments for each of the three movement conditions (PASSIVE, ASSISTED and ACTIVE movement) were averaged for each single subject. All three conditions of one subject were normalized to the maximum EMG activity obtained during the ACTIVE condition of a given subject. Finally, the normalized EMG curves of all subjects were averaged, and the mean activities were analyzed. We performed an ANOVA and a post-hoc Bonferroni–Holm corrected *t*-test on paired samples, applying the correction procedure that Holm (1979) suggested. This procedure refers to a step-down method based on the classical Bonferroni correction for multiple comparisons. *T*-values were reported as being significant only if the corresponding *p*-value survived the correction procedure characterized by the initial *p*-value of 0.05 and the number of tests.

Results

EMG analysis

EMG signals recorded from the rectus femoris, biceps femoris, tibialis anterior and gastrocnemius medialis of the left leg during the experimental movement period and during the two conditions ACTIVE and PASSIVE showed clearly distinguishable patterns. The upper panel of Fig. 3 shows the chronological sequence of the EMG activity of the muscle rectus femoris during one gait cycle ($n = 8$). The PASSIVE condition led to an EMG signal close to zero, whereas the ACTIVE one demonstrates strong

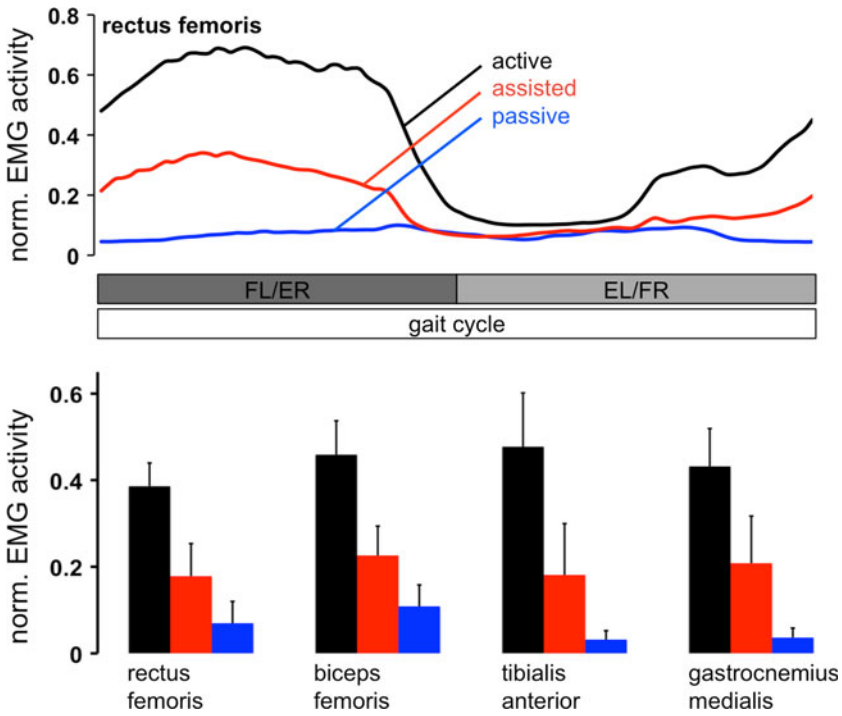

Fig. 3 Chronological sequence of the normalized EMG activity of the muscle rectus femoris during one gait cycle (*upper panel*). Averaged EMG activity of the whole gait cycle of the muscle rectus femoris, biceps femoris, tibialis anterior as well as gastrocnemius medialis (*lower panel*). All data are based on 8 subjects

Table 1 Results of the paired *t*-test (one-tailed) regarding the mean differences of the activity level between ACTIVE, ASSISTED and PASSIVE condition

Muscles	Comparison	
	ACTIVE > ASSISTED	ASSISTED > PASSIVE
Rectus femoris	$t(df = 7) = 7.274$; $p < 0.001$	$t(df = 7) = 4.694$; $p = 0.001$
Biceps femoris	$t(df = 7) = 7.155$; $p < 0.001$	$t(df = 7) = 4.805$; $p = 0.001$
Tibialis anterior	$t(df = 7) = 6.379$; $p < 0.001$	$t(df = 7) = 3.544$; $p = 0.005$
Gastrocnemius medialis	$t(df = 7) = 11.182$; $p < 0.001$	$t(df = 7) = 4.244$; $p = 0.002$

All comparisons survived the significance criterion of the Bonferroni–Holm procedure with an initial p threshold of 0.05

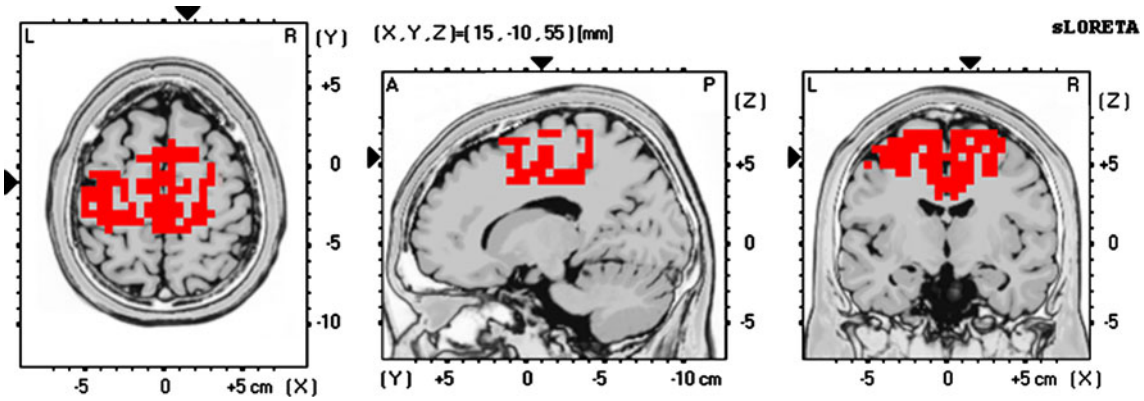

Fig. 4 Source localization of the movement-related potential in relation to the spontaneous EEG activity in the resting periods of all subjects ($n = 20$). For the analysis, averaged data of the whole gait cycle (0–2750 ms) were used

activity. The EMG activity pattern recorded during the experimental, uninstructed movement period (labeled "ASSISTED" in Fig. 3) was of lower amplitude but very similar to the one recorded during the ACTIVE condition.

The difference in the temporal course of muscle activity is expressed via the averaged EMG activity of the whole gait cycle (Fig. 3, lower panel). In addition to the rectus femoris, all muscles show a similar ratio of activity between ACTIVE, ASSISTED and PASSIVE condition. Between-condition differences regarding the activity level are significant for all four muscles (ANOVAs, $p < 0.01$). Post-hoc *t*-tests, corrected for multiple comparisons, showed that muscular activity was highest during the ACTIVE condition, followed by the ASSISTED and the PASSIVE conditions (see also Table 1).

Spectral alpha- and beta-power

The spectral analysis of the alpha band as well as the beta band revealed significantly higher mean power values during the resting periods compared to the movement period (paired *t*-test on normal distributed log-transformed data, $p < 0.005$). Expressed in percent, the mean alpha power at the pooled Cz and CPz electrodes drops about 68.16% (SE: ± 4.62%) and the mean beta power drops about 35.45% (SE: ± 16.02%) during *Erigo*-assisted leg movement.

Source localization

With help of sLORETA, source localization was performed to identify areas active during the *Erigo*-assisted leg movements (Fig. 4). For one gait cycle (0–2750 ms), the comparison between the underlying sources of movement-related potentials and spontaneous EEG during the resting periods resulted in 680 significant voxels (out of 6239 voxels with a size of 5 × 5 × 5 mm; $p < 0.0005$).

As displayed in Table 2, most active voxels (51.6%) are located in classical motor regions such as M1, PMC and SMA. Thirty-two percent among the active voxels are encountered in the CC which is also considered being part of the motor system. Further active structures are the primary sensory cortex (S1, 12.4%) and the SA (4.0%).

Movement-related potentials: temporal patterns

The eight scalp maps, created to represent the average gait cycle, demonstrated temporal changes of the potential differences across time (Fig. 5). In general, the scalp maps showed a positive potential at fronto-central locations and a

Table 2 Significant active cortical areas of movement-related potential in relation to the spontaneous EEG activity in the resting periods ($p < 0.0005$)

Functional areas	BA	# Voxels
Primary somatosensory cortex (S1)	1, 2, 3	84
Primary motor cortex (M1)	4	66
Somatosensory association cortex (SA)	5, 7	27
Premotor cortex (PMC) & Supplementary motor cortex (SMA)	6	285
Cingulate cortex (CC)	23, 31 24, 32	218

Table 3 Significant active cortical areas during time intervals of 50 ms of the movement-related potential in relation to the spontaneous EEG activity in the resting periods ($p < 0.001$)

Functional areas	BA	# Voxels				
		Period A	Period B	Period C	Period D	Period E
S1	1, 2, 3	–	–	–	21	17
M1	4	10	–	–	24	28
SA	5, 7	–	–	–	–	42
PMC & SMA	6	105	47	130	146	186
CC	23, 31 24, 23	–	56	144	146	142
Total		115	103	274	337	415

Periods A–E are related to Fig. 7, and the corresponding time intervals are 383–433 ms (period A), 592–642 ms (period B), 772–822 ms (period C), 924–974 ms (period D) and 1182–1232 ms (period E)

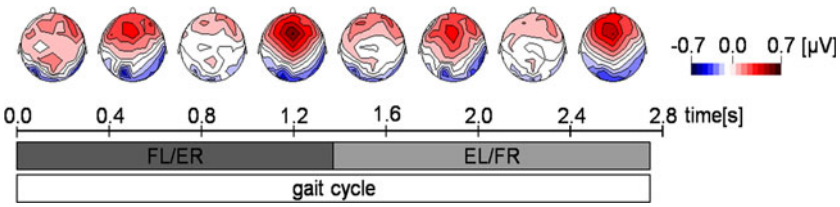

Fig. 5 Eight scalp maps of the averaged movement-related potential of all subjects ($n = 20$)

negative potential at parieto-occipital spots. Recurrent patterns were observed by analyzing the sequence of the eight maps. Focusing on the first half of the gait cycle (maps 1–4), there was high global activity in the second and fourth map compared to map 1 and 3. Furthermore, by visual inspection, strong similarities between the maps from the first (FL/ER, maps 1–4) and second (EL/FR, maps 5–8) half of the gait cycle were observed. The temporal patterns of the first half are qualitatively equal to the patterns of the second half (map 1 corresponds to map 5, map 2 with map 6 and so on).

During the whole gait cycle (0.00–2.75 s), the movement-related potential at the Cz electrode had a highly periodic shape and higher amplitudes compared to the activity during the two resting periods (Fig. 6). The flexion of the left leg (FL) and the extension of the right leg (ER) took place in the first half of the gait cycle (0.00–1.375 s), whereas the extension of the left leg (EL) and the flexion of the right leg (FR) are performed in the second half (1.375–2.75 s). The temporal course of the movement-related potential can be divided into two equal parts corresponding to the FL/ER and EL/FR. As obvious from Fig. 6 (right panel), superimposing the two phases did not lead to significant differences between the two curves ($p > 0.05$).

Finally, the averaged movement-related potential of the two superimposed periods of the gait cycle (FL/ER and EL/FR) is shown in Fig. 7. Applying a *t*-test on log-transformed data against rest periods, we identified five significant peaks of the movement-related potential. Each scalp map represents the average activity of a 50-ms time interval related to one of the five significant peaks A–E ($p < 0.001$). The scalp map for period E shows the overall strongest positive potential, whereas the scalp map at period C illustrates a distinct negative one.

Source localization at these five intervals demonstrates a strong activation of PMC and SMA during all time periods Table 3. However, significant voxels at M1 can only be found in period A, D and E. Period B and C show activation in the CC but no significant activity in S1, M1 and SA. The strongest overall activation in terms of number of significant voxels can be seen in period E. Period D shows the same activated areas as period E with SA as an exception and less amount of total significant voxels.

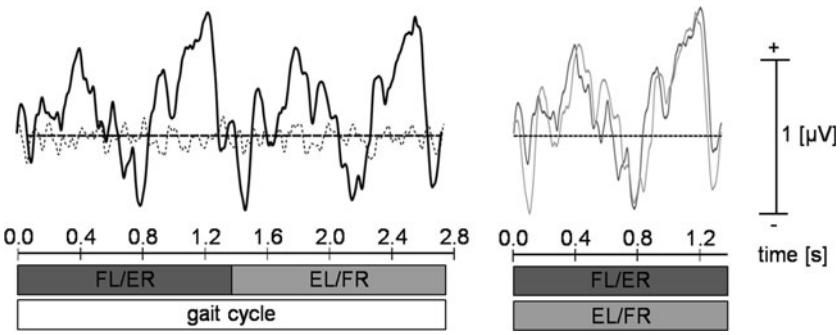

Fig. 6 Averaged movement-related potential *(solid line, left graph)* of all subjects ($n = 20$) at the Cz electrode compared to the activity during the two averaged resting periods *(dotted line, left graph)*. The *left graph* illustrates a whole gait cycle while the *right* one shows the two periods of gait cycle (FL/ER and EL/FR) superimposed

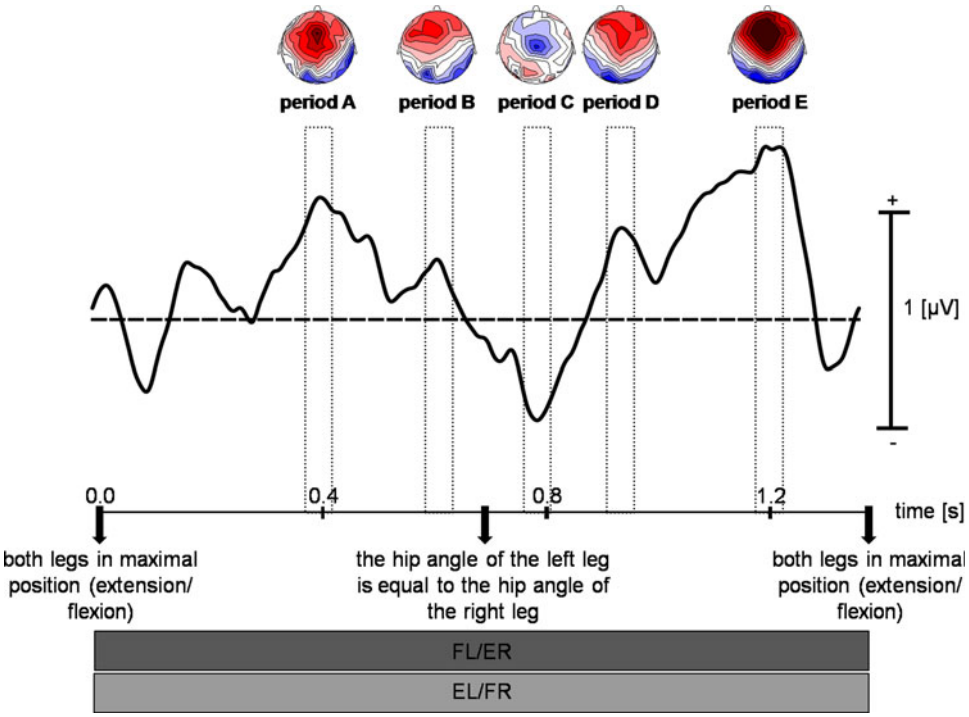

Fig. 7 Averaged movement-related potential of FL/ER and EL/FR at the Cz electrode (see also *right graph* of Fig. 6). Each scalp map represents the average activity of the below marked time period (duration: 50 ms) related to one of the five significant peaks ($p < 0.001$)

Discussion

Cortical activity during rhythmic leg movement was investigated with assistance of the dynamic tilt table *Erigo*. Providing the guidance of the *Erigo*, all subjects were able to perform equal and standardized movements. Initially performed global analyses of movement-induced cortical activity revealed an expected network of primary and secondary sensorimotor areas.

EMG activity and stepping movements

Performing the *Erigo*-assisted gait-like leg movement (ASSISTED), EMG measurements revealed a muscular activity pattern that was of lower intensity but very similar to the ACTIVE condition, where the subjects were instructed to actively participate in the movement. On the contrary, EMG activity during PASSIVE condition is only associated with some muscle activity due to reflexes and therefore, it was significantly lower compared to the ASSISTED condition. The *Erigo* allows a highly synchronized movement between the hip, knee and ankle joints of the left and right leg. Like during human walking, both legs move concurrent but in converse directions to each other. At the end of the extension phase, a ground reaction force arises which is comparable to heel strike and stand phase. Nevertheless, the assisted gait-like leg movement is only performed at a defined location, and therefore, there is no movement in a walking direction. In conclusion, the assisted gait-like leg movement is a compromise between real human walking, reduction in movement artifacts and standardized leg movement that seems appropriate for investigating the neural underpinnings of human gait.

To get an additional proof that EEG activity reflects motor and sensory aspects of cortical processing, an analysis of movement-induced alpha and beta power depression (TRPD) at electrodes overlying the primary sensorimotor

leg area (Cz and CPz) was performed. As reported from other research groups (Hummel and Gerloff 2006; Neuper et al. 2006), this observation is related to a long-lasting activation of neuronal networks in sensorimotor areas. As we showed a decrease in these power bands, we can confirm that the gait-like leg movement in the Erigo yields to motor as well as sensory aspects of cortical processing.

Impact for neurorehabilitation

We revealed gait-associated activations primarily in the primary (M1) and secondary motor areas (SMA, PMC, CC) as well as in S1 and sensory association areas. Therefore, we assume that an *Erigo*-assisted rehabilitation therapy also activates brain regions classically associated with human gait. Especially from a therapeutic point of view, this is a crucial observation. Like in the study of Bernhardt et al. (2007), A Very Early Rehabilitation Trail (AVERT) would be possible and safe via the *Erigo*. In this study, they showed an absolute 9% trend toward benefit in patients with stroke who engaged in early, intensive rehabilitation compared with those who did not. An additional selective activation of the neuronal circuits involved in gait may enhance this effect and lead to an even better outcome. To verify this, further studies are needed. Nevertheless, our findings are of particular importance for new and improved approaches in the field of neurorehabilitation.

Evaluation of findings

So far, only very few SPECT and NIRS studies analyzed brain structures involved during human walking in detail. Excluding subcortical brain structures, Fukuyama et al. (1997) and Miyai et al. (2001) identified M1, S1 and SMA as active cortical areas. Hanakawa et al. (1999a, b) as well as this present study found an expanded cortical network comprising the PMC, the SA and the CC in addition to the previous mentioned structures. So, our results generally are in very good agreement with these studies.

Due to well-known limitations of the EEG method, activity in subcortical brain structures could not be considered in the present study. Therefore, we were not able to replicate activations in the striatum, cerebellum, pons and basal ganglia that have been identified in two previous SPECT studies (Fukuyama et al. 1997; Hanakawa et al. 1999a, b). Furthermore, low spatial resolution is a drawback of the EEG/sLORETA technique. This is particularly relevant for the leg motor area, since its medial location causes a very small spatial distance between the leg areas of the left and the right hemisphere. Hence, we were not able to assess hemispheric differences related to the different activities of the left and right leg at different time points of the gait cycle.

In contrast to that, the chosen method has the advantage of a high temporal resolution. This gives us the opportunity to analyze changes in neural activity associated with the gait cycle and its different phases.

Movement-related potentials: temporal aspects

Overall, the scalp topographies showed a characteristic pattern of positive potential differences at fronto-central locations and negative ones at parieto-occipital spots. Comparing the two mirror-inverted phases of the gait cycle (FL/ER and EL/FL), a very similar temporal sequence of scalp maps was recognized. Additionally, based on our EEG recordings at the Cz electrode, there was no significant difference between the neuronal activity pattern of the first and second half of the gait cycle. In part, these two observations may be related to the above-mentioned problem of low spatial resolution with respect to the leg motor area. However, due to the lack of differences, we averaged both phases of the gait cycle in a next step and analyzed the resulting average activity. At the beginning as well as at the end of the averaged half gait cycle (duration: 1.375 s), the right and left leg are in a maximal position (flexion or extension, respectively). In the middle of this period, the hip angle of both legs is equal and represents the only time point at which the legs are concurrently at the same position.

Focusing on the intensity of cortical activity as indicated by the amplitudes of the evoked movement potential, strongest activity was found shortly before both legs are at maximal position (flexion/extension). As known from simple finger tapping, which can also been described as elementary, rhythmic movement pattern, the most time-consuming and neuronal costly aspect lies in the phase where the finger changes direction. It has been shown that the actual travel time of the finger between the two reversal-of-direction points only represents a very minor portion of the time taken by one complete up-and-down beat cycle of the finger (Peters 1980; Koeneke et al. 2009). Following this evidence, a training-induced gain in tapping speed, as demonstrated in a recent study by Koeneke et al. (2009), must of necessity derive from more efficient and faster change from the flexor to extensor activation (and vice versa) during the reversal of movement direction. Transferring these results to our leg movement (extension and flexion), we assume that the process of changing the movement direction demands the highest neural control within the involved cortical network.

Conclusion & Outlook

The present study provides further indication to the notion that the S1, M1 and SMA play an essential role in cortical

control of human gait. PMC, cingulated cortical areas and the SA are highly involved in this complex process. Furthermore, the temporal analysis suggests the existence of a direct relation between performed movement and measured cortical activation. Based on our results, we conclude that within the gait cycle, most cortical capacity is needed for the process of changing the direction between the flexor and extensor movement.

The activated brain regions during the rhythmic gait-like leg movement are all classically associated with human gait. These findings are invaluable from a therapeutic point of view. An enhanced understanding of the human gait will provide the basis to improve and shorten the rehabilitation process.

Further experiments and analyses are necessary to map temporal and spatial patterns of cortical activation to real human gait. This would be of major interest for many other applications in the field of neurorehabilitation or brain–computer interfaces. Detected signals can be feed into a controller that drives neuroprostheses based on the patient's intentions. Alternatively, training in a virtual environment may provide new promising opportunities.

Acknowledgments This work was supported by the National Center of Competence in Research (NCCR) on Neural Plasticity and Repair funded by the Swiss National Foundation (SNF). Special thanks to Gery Colombo, Jan Lichtenberg, Barbara Jost and Roger Gassert for their technical support as well as Clemens Gutknecht, Josef Ludwig Schönberger, Daniel Zutter and Romy Rodriguez del Rio for their clinical support during the study.

References

Andres FG, Mima T, Schulman AE, Dichgans J, Hallett M, Gerloff C (1999) Functional coupling of human cortical sensorimotor areas during bimanual skill acquisition. Brain 122:855–870

Armstrong DM (1988) The supraspinal control of mammalian locomotion. J Physiol Lond 405:1–37

Bernhardt J, Dewey H, Collier J, Thrift A, Sharpley T, Donnan G (2007) A very early rehabilitation trial (AVERT) phase II safety and feasibility results. Stroke 38:473

Ciccarelli O, Toosy AT, Marsden JF, Wheeler-Kingshott CM, Sahyoun C, Matthews PM, Miller DH, Thompson AJ (2005) Identifying brain regions for integrative sensorimotor processing with ankle movements. Exp Brain Res 166:31–42

Dietz V (2003) Spinal cord pattern generators for locomotion. Clin Neurophysiol 114:1379–1389

Dittmar M (2002) Functional and postural lateral preferences in humans: interrelations and life-span age differences. Hum Biol 74:569–585

Dobkin BH, Firestine A, West M, Saremi K, Woods R (2004) Ankle dorsiflexion as an fMRI paradigm to assay motor control for walking during rehabilitation. Neuroimage 23:370–381

Duysens J, Van de Crommert HWAA (1998) Neural control of locomotion; Part 1. The central pattern generator from cats to humans. Gait Posture 7:131–141

Fukuyama H, Ouchi Y, Matsuzaki S, Nagahama Y, Yamauchi H, Ogawa M, Kimura J, Shibasaki H (1997) Brain functional activity during gait in normal subjects: a SPECT study. Neurosci Lett 228:183–186

Gerloff C, Richard J, Hadley J, Schulman AE, Honda M, Hallett M (1998) Functional coupling and regional activation of human cortical motor areas during simple, internally paced and externally paced finger movements. Brain 121(Pt 8):1513–1531

Hanakawa T (2006) Neuroimaging of standing and walking: special emphasis on Parkinsonian gait. Parkinsonism Relat Disord 12:S70–S75

Hanakawa T, Fukuyama H, Katsumi Y, Honda M, Shibasaki H (1999a) Enhanced lateral premotor activity during paradoxical gait in Parkinson's disease. Ann Neurol 45:329–336

Hanakawa T, Katsumi Y, Fukuyama H, Honda M, Hayashi T, Kimura J, Shibasaki H (1999b) Mechanisms underlying gait disturbance in Parkinson's disease: a single photon emission computed tomography study. Brain 122(Pt 7):1271–1282

Harada T, Miyai I, Suzuki M, Kubota K (2009) Gait capacity affects cortical activation patterns related to speed control in the elderly. Exp Brain Res 193:445–454

Holm S (1979) A simple sequentially rejective multiple test procedure. Scand J Stat 6:65–70

Hummel FC, Gerloff C (2006) Interregional long-range and short-range synchrony: a basis for complex sensorimotor processing. Prog Brain Res 159:223–236

Hummel F, Andres F, Altenmuller E, Dichgans J, Gerloff C (2002) Inhibitory control of acquired motor programmes in the human brain. Brain 125:404–420

Iseki K, Hanakawa T, Hashikawa K, Tomimoto H, Nankaku M, Yamauchi H, Hallett M, Fukuyama H (2010) Gait disturbance associated with white matter changes: a gait analysis and blood flow study. Neuroimage 49:1659–1666

Jahn K, Deutschlander A, Stephan T, Strupp M, Wiesmann M, Brandt T (2004) Brain activation patterns during imagined stance and locomotion in functional magnetic resonance imaging. Neuroimage 22:1722–1731

Koeneke S, Battista C, Jaencke L, Peters M (2009) Transfer effects of practice for simple alternating movement. J Mot Behav (in press)

Malouin F, Richards CL, Jackson PL, Dumas F, Doyon J (2003) Brain activations during motor imagery of locomotor-related tasks: a PET study. Hum Brain Mapp 19:47–62

Manganotti P, Gerloff C, Toro C, Katsuta H, Sadato N, Zhuang P, Leocani L, Hallett M (1998) Task-related coherence and task-related spectral power changes during sequential finger movements. Electroencephalogr Clin Neurophysiol 109:50–62

Miyai I, Tanabe HC, Sase I, Eda H, Oda I, Konishi I, Tsunazawa Y, Suzuki T, Yanagida T, Kubota K (2001) Cortical mapping of gait in humans: a near-infrared spectroscopic topography study. NeuroImage 14:1186–1192

Miyai I, Yagura H, Oda I, Konishi I, Eda H, Suzuki T, Kubota K (2002) Premotor cortex is involved in restoration of gait in stroke. Ann Neurol 52:188–194

Miyai I, Yagura H, Hatakenaka M, Oda I, Konishi I, Kubota K (2003) Longitudinal optical imaging study for locomotor recovery after stroke. Stroke 34:2866–2870

Neuper C, Wortz M, Pfurtscheller G (2006) ERD/ERS patterns reflecting sensorimotor activation and deactivation. Prog Brain Res 159:211–222

Pascual-Marqui RD (2002) Standardized low-resolution brain electromagnetic tomography (sLORETA): technical details. Methods Find Exp Clin Pharmacol 24(Suppl D):5–12

Pascual-Marqui RD, Lehmann D, Koenig T, Kochi K, Merlo MC, Hell D, Koukkou M (1999) Low resolution brain electromagnetic tomography (LORETA) functional imaging in acute, neuroleptic-naive, first-episode, productive schizophrenia. Psychiatry Res 90:169–179

Pascual-Marqui RD, Esslen M, Kochi K, Lehmann D (2002) Functional imaging with low-resolution brain electromagnetic tomography (LORETA): a review. Methods Find Exp Clin Pharmacol 24:91–95

Peters M (1980) Why the preferred hand taps more quickly than the non-preferred hand—3 experiments on handedness. Can J Psychology-Revue Canadienne De Psychologie 34:62–71

Sacco K, Cauda F, Cerliani L, Mate D, Duca S, Geminiani GC (2006) Motor imagery of walking following training in locomotor attention—The effect of 'the tango lesson'. Neuroimage 32:1441–1449

Sahyoun C, Floyer-Lea A, Johansen-Berg H, Matthews PM (2004) Towards an understanding of gait control: brain activation during the anticipation, preparation and execution of foot movements. Neuroimage 21:568–575

Suzuki M, Miyai I, Ono T, Oda I, Konishi I, Kochiyama T, Kubota K (2004) Prefrontal and premotor cortices are involved in adapting walking and running speed on the treadmill: an optical imaging study. Neuroimage 23:1020–1026

Suzuki M, Miyai I, Ono T, Kubota K (2008) Activities in the frontal cortex and gait performance are modulated by preparation. An fNIRS study. Neuroimage 39:600–607

Talairach J, Tournoux P (eds) (1988) Co-planar stereotaxic atlas of the human brain. Thieme, Stuttgart

Yazawa S, Shibasaki H, Ikeda A, Terada K, Nagamine T, Honda M (1997) Cortical mechanism underlying externally cued gait initiation studied by contingent negative variation. Electroencephalogr Motor Control Electroencephalogr Clin Neurophysiol 105:390–399